

Effect of non-zero θ_{13} on the measurement of θ_{23}

Sushant K. Raut*

Physical Research Laboratory, Ahmedabad, India

(Dated: April 15, 2019)

Abstract

The moderately large measured value of θ_{13} signals a departure from the approximate two-flavour oscillation framework. As a consequence, the relation between the value of θ_{23} in nature, and the mixing angle measured in ν_μ disappearance experiments is non-trivial. In this paper, we calculate this relation analytically. We also derive the correct conversion between degenerate values of θ_{23} in the two octants. Through simulations of a ν_μ disappearance experiment, we show that there are observable consequences of not using the correct relation in calculating oscillation probabilities. These include a wrong best-fit value for θ_{23} , and spurious sensitivity to the octant of θ_{23} .

PACS numbers: 14.60.Pq, 14.60.Lm, 13.15.+g

Keywords: Atmospheric mixing angle, Octant degeneracy, Long Baseline Experiments

*Email Address: sushant@prl.res.in

I. INTRODUCTION

Neutrino oscillation physics has entered an era of precision measurements. Since 2011, the reactor experiments Daya Bay [1], Double Chooz [2, 3] and RENO [4] and superbeam experiments MINOS [5] and T2K [6] have measured a non-zero value of θ_{13} [7–9]. Analyses of world neutrino data [10–12] have given us the value $\sin^2 2\theta_{13} \simeq 0.1$, which is moderately large. Daya Bay has measured $\sin^2 2\theta_{13} = 0.089 \pm 0.011$ [13], which is the most precise measurement till date. These measurements have established that θ_{13} is non-zero at more than 5σ confidence level.

The solar mixing angle θ_{12} and mass-squared difference Δ_{21} ($\Delta_{ij} = m_i^2 - m_j^2$) have been measured very accurately by SNO [14] and KamLAND [15], respectively. Their current best-fit values are $\sin^2 \theta_{12} = 0.32 \pm 0.017$ and $\Delta_{21} = (7.62 \pm 0.2) \times 10^{-5} \text{eV}^2$ [10]. MINOS [5] has measured the mixing angle $\theta_{\mu\mu}$ and mass-squared difference $\Delta_{\mu\mu}$ with a precision of a few percent. We use the subscript $\mu\mu$ to indicate that these parameters are measured from observations of muon neutrino disappearance. The values of these parameters from MINOS are $\sin^2 2\theta_{\mu\mu} > 0.90$ (90% C.L.) and $|\Delta_{\mu\mu}| = (2.32 \pm 0.1) \times 10^{-3} \text{eV}^2$ [16]. In the two-flavour oscillation scenario (neglecting the small parameters Δ_{21} and θ_{13}), the muon neutrino survival probability $P_{\mu\mu}$ depends on $\sin^2 2\theta_{\mu\mu} = \sin^2 2\theta_{23}$ and $|\Delta_{\mu\mu}| = |\Delta_{31}|$. Because this probability depends on the magnitude but not the sign of $|\Delta_{31}|$, we cannot determine the neutrino mass ordering or hierarchy. Moreover, this function is symmetric about $\theta_{23} = 45^\circ$, which gives rise to the octant degeneracy. Thus, the currently unknown parameters in standard three-flavour neutrino oscillation physics are - (a) the neutrino mass hierarchy (normal hierarchy (NH): $\Delta_{\mu\mu} > 0$ or inverted hierarchy (IH): $\Delta_{\mu\mu} < 0$), (b) the CP-violating phase δ_{CP} and (c) the octant of $\theta_{\mu\mu}$ (lower octant (LO): $\theta_{\mu\mu} < 45^\circ$ or higher octant (HO): $\theta_{\mu\mu} > 45^\circ$).

It is possible for the mass hierarchy to be determined by the upcoming experiment NO ν A itself, if the value of δ_{CP} in nature is in the favourable range [17]. Combined data from multiple experiments [18–20], experiments with longer baselines [21, 22] and atmospheric neutrino experiments [23, 24] can also determine the hierarchy. The measurement of δ_{CP} is difficult but possible, thanks to the non-zero value of θ_{13} . This requires very intense beams at short baselines [25]. In this work, we concentrate on the precision measurement of the atmospheric mixing angle.

θ_{23} is the largest of the mixing angles in the leptonic and quark sectors. Its near-maximal value is indicative of a symmetry of nature in the $\mu - \tau$ sector [26, 27]. In many theoretical models, the deviation of θ_{23} from maximality is related to the deviation of θ_{13} from zero [27]. Thus, the precision measurement of this angle, and determination of its octant can play an important role in constructing new models of physics.

In this paper, we discuss the measurement of θ_{23} and its octant, particularly in light of moderately large θ_{13} , which gives rise to three-flavour effects. In Ref. [28, 29], the authors had shown that due to three-flavour effects, the mass-squared difference $\Delta_{\mu\mu}$ measured in muon disappearance experiments is not Δ_{31} , but a linear combination of Δ_{31} and Δ_{21} . The same calculation also indicates that the mixing angle $\theta_{\mu\mu}$ measured in these experiments is not the same as θ_{23} . While this result has been seen in the literature before (in Ref. [30]) and more recently in Ref. [12], we present a detailed study of this effect in this paper. We pay particular attention to the effect of choosing the ‘wrong’ definition ($\theta_{23} = \theta_{\mu\mu}$) in analyses. In Section II, we have outlined the calculation that indicates the relation between $\Delta_{\mu\mu}, \theta_{\mu\mu}$ and Δ_{31}, θ_{23} . We have also found analytic expressions relating deviations from maximality in the two octants. In this work, our aim is to highlight a physics point, rather than study the capability of any particular experiment. However, in order to make our point clearer, we have presented the results of some simulations, in Section III. Finally, in Section IV, we have summarized our findings.

II. CALCULATIONS

The $P_{\mu\mu}$ oscillation probability in the three-flavour scenario (ignoring matter effects) is given by

$$\begin{aligned}
P_{\mu\mu} = 1 & - 4|U_{\mu 3}|^2|U_{\mu 1}|^2 \sin^2 \hat{\Delta}_{31} \\
& - 4|U_{\mu 3}|^2|U_{\mu 2}|^2 \sin^2 \hat{\Delta}_{32} \\
& - 4|U_{\mu 2}|^2|U_{\mu 1}|^2 \sin^2 \hat{\Delta}_{21} ,
\end{aligned} \tag{1}$$

where we have used the shorthand notation $\hat{\Delta}_{ij} = \Delta_{ij}L/4E$. Here, $U_{\alpha i}$ are the elements of the 3×3 PMNS matrix. This probability is sensitive to all six standard oscillation parameters - three mixing angles, two mass-squared differences and the CP phase. In interpreting the result of oscillation data in terms of two-flavour oscillations, we attempt to express the

probability in the simple form

$$P_{\mu\mu} = 1 - \sin^2 2\theta_{\mu\mu} \sin^2 \hat{\Delta}_{\mu\mu} \quad (2)$$

that involves only two parameters. Recasting the full six-parameter formula as a simple two-parameter formula results in a non-trivial relation between $\Delta_{\mu\mu}$ and Δ_{31} , and between $\theta_{\mu\mu}$ and θ_{23} . In this calculation, we will consistently retain only terms upto linear order in Δ_{21} (since $\Delta_{21} \ll \Delta_{31}$). Ignoring the last term in Eq. 1, we have

$$\frac{1 - P_{\mu\mu}}{4} = |U_{\mu 3}|^2 |U_{\mu 1}|^2 \sin^2 \hat{\Delta}_{31} + |U_{\mu 3}|^2 |U_{\mu 2}|^2 \sin^2 \hat{\Delta}_{32} . \quad (3)$$

Here we introduce the notation

$$u_1 = \frac{|U_{\mu 1}|^2}{|U_{\mu 1}|^2 + |U_{\mu 2}|^2} , \quad u_2 = \frac{|U_{\mu 2}|^2}{|U_{\mu 1}|^2 + |U_{\mu 2}|^2} .$$

Note that $u_1 + u_2 = 1$. This notation lets us write

$$\frac{1 - P_{\mu\mu}}{4} = |U_{\mu 3}|^2 (|U_{\mu 1}|^2 + |U_{\mu 2}|^2) \left(u_1 \sin^2 \hat{\Delta}_{31} + u_2 \sin^2 \hat{\Delta}_{32} \right) . \quad (4)$$

Using the fact that $\Delta_{32} = \Delta_{31} - \Delta_{21}$, a little algebra gives us

$$\frac{1 - P_{\mu\mu}}{4} = \frac{1}{2} |U_{\mu 3}|^2 (|U_{\mu 1}|^2 + |U_{\mu 2}|^2) \left[1 - \cos 2\hat{\Delta}_{31} - 2u_2 \hat{\Delta}_{21} \sin 2\hat{\Delta}_{31} \right] . \quad (5)$$

We rewrite this as

$$\begin{aligned} \frac{1 - P_{\mu\mu}}{4} &= \frac{1}{2} |U_{\mu 3}|^2 (|U_{\mu 1}|^2 + |U_{\mu 2}|^2) \\ &\quad \left[1 - \left(\cos \beta \cos 2\hat{\Delta}_{31} + \sin \beta \sin 2\hat{\Delta}_{31} \right) \sqrt{1 + 4u_2^2 \hat{\Delta}_{21}^2} \right] \\ &= \frac{1}{2} |U_{\mu 3}|^2 (|U_{\mu 1}|^2 + |U_{\mu 2}|^2) \left[1 - \cos(2\hat{\Delta}_{31} - \beta) \sqrt{1 + 4u_2^2 \hat{\Delta}_{21}^2} \right] . \end{aligned} \quad (6)$$

where

$$\cos \beta = \frac{1}{\sqrt{1 + 4u_2^2 \hat{\Delta}_{21}^2}} , \quad \sin \beta = \frac{2u_2 \hat{\Delta}_{21}}{\sqrt{1 + 4u_2^2 \hat{\Delta}_{21}^2}} .$$

We ignore the quadratic term in the square root, and we note that $\beta = \tan^{-1}(2u_2 \hat{\Delta}_{21}) \approx 2u_2 \hat{\Delta}_{21}$. This gives us our final result

$$P_{\mu\mu} = 1 - 4|U_{\mu 3}|^2 (1 - |U_{\mu 3}|^2) \sin^2(\hat{\Delta}_{31} - u_2 \hat{\Delta}_{21}) . \quad (7)$$

On comparing with the two-flavour formula, we can make the association

$$\Delta_{31} = \Delta_{\mu\mu} + u_2 \Delta_{21} ,$$

which is the result expressed in Ref. [28]. Moreover, we also find that

$$\begin{aligned} \sin^2 2\theta_{\mu\mu} &= 4|U_{\mu 3}|^2 (1 - |U_{\mu 3}|^2) \\ &= 4 \cos^2 \theta_{13} \sin^2 \theta_{23} (1 - \cos^2 \theta_{13} \sin^2 \theta_{23}) . \end{aligned}$$

This means that

$$\sin \theta_{23} = \sin \theta_{\mu\mu} / \cos \theta_{13} \quad \text{or} \quad \sin \theta_{23} = \sin(90^\circ - \theta_{\mu\mu}) / \cos \theta_{13} . \quad (8)$$

In other words, given a value of $\sin^2 2\theta_{\mu\mu}$, there are two degenerate allowed values of $\theta_{\mu\mu}$: $\theta_{\mu\mu}^{LO}$ (in the lower octant) and $\theta_{\mu\mu}^{HO}$ (in the higher octant). These are related by

$$\theta_{\mu\mu}^{LO} = 90^\circ - \theta_{\mu\mu}^{HO} . \quad (9)$$

Then, the corresponding values of θ_{23} are given by

$$\sin \theta_{23}^{LO} = \frac{\sin \theta_{\mu\mu}^{LO}}{\cos \theta_{13}} \quad ; \quad \sin \theta_{23}^{HO} = \frac{\sin \theta_{\mu\mu}^{HO}}{\cos \theta_{13}} . \quad (10)$$

Thus, if $\theta_{13} = 0$, we have simply $\theta_{23}^{LO} = \theta_{\mu\mu}^{LO}$ and $\theta_{23}^{HO} = \theta_{\mu\mu}^{HO}$. However, for non-zero θ_{13} , the relation between θ_{23}^{LO} and θ_{23}^{HO} depends on the value of θ_{13} .

We have shown this feature in Fig. 1. Along the x-axis, we have different values of $\sin^2 2\theta_{\mu\mu}$ as measured using the $P_{\mu\mu}$ channel. For a particular value of θ_{13} , each $\theta_{\mu\mu}$ corresponds to two values of θ_{23} . These two values have been plotted along the y-axis. Thus given a value of θ_{13} we have a curve that maps one value of $\theta_{\mu\mu}$ to two values of θ_{23} . To show the effect of θ_{13} , we have varied it in the range $\sin^2 2\theta_{13} \in [0.0, 0.2]$. The solid black curve is for $\sin^2 2\theta_{13} = 0.1$. The spread in θ_{13} gives the shaded band in the figure.

The main point to be noted here is the asymmetry of the band about the $\theta_{23} = 45^\circ$ line. When $\sin^2 2\theta_{13} = 0$, we see that the curve is symmetric about $\theta_{23} = 45^\circ$. However, for larger values of θ_{13} such as $\sin^2 2\theta_{13} = 0.2$, we lose this symmetry. For instance, if $\sin^2 2\theta_{13} = 0.2$ and if the MINOS measured value of $\sin^2 2\theta_{\mu\mu} = 0.98$, then the values of θ_{23} in the two octants are 40.5° and 52.7° . These two angles are not complementary. In other words, it is $\theta_{\mu\mu}$ that goes to $90 - \theta_{\mu\mu}$ under the octant degeneracy; but θ_{23}^{LO} and θ_{23}^{HO} are not complementary angles - the exact change depends on the value of θ_{13} . Henceforth, for

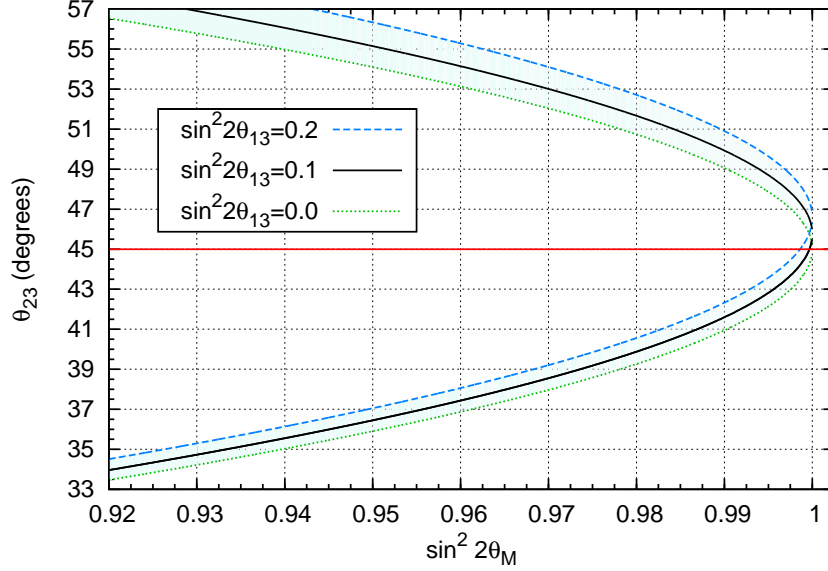


FIG. 1: Allowed values for θ_{23} (y-axis) in degrees, for a given measurement of $\sin^2 2\theta_{\mu\mu}$ (x-axis). The dashed (blue) and dotted (green) curves are for the extreme cases $\sin^2 2\theta_{13} = 0.2$ and 0.0 , respectively. The solid (black) curve is for $\sin^2 2\theta_{13} = 0.1$.

convenience, we will refer to θ_{23}^{LO} and θ_{23}^{HO} corresponding to a given measurement of $\sin^2 2\theta_{\mu\mu}$ as being μ -complementary .

As an interesting aside, we note that (given $\sin^2 2\theta_{13} = 0.1$) if $44.3^\circ < \theta_{\mu\mu} < 45.7^\circ$, i.e. if $\sin^2 2\theta_{\mu\mu} > 0.9993$, then both allowed values of θ_{23} are greater than 45° . In such a case, there is no ambiguity in the octant of θ_{23} – it is necessarily in the higher octant. However, current experiments do not have the precision to distinguish $\sin^2 2\theta_{\mu\mu} = 0.9993$ from $\sin^2 2\theta_{\mu\mu} = 1$. Therefore, this point is purely of academic interest.

Hereafter, we assume that $\sin^2 2\theta_{13} = 0.1$. When $\sin^2 2\theta_{\mu\mu} = 1.0$, i.e. $\theta_{\mu\mu}^{LO} = \theta_{\mu\mu}^{HO} = 45^\circ$, we get $\theta_{23}^{LO} = \theta_{23}^{HO} = 45.75^\circ$ from Eq. 10. This is also seen from Fig. 1. For a given value of $\sin^2 2\theta_{\mu\mu} \neq 1.0$, the two allowed values of $\theta_{\mu\mu}$ have equal and opposite deviations from 45° , i.e. $\theta_{\mu\mu}^{LO} < 45^\circ$ and $\theta_{\mu\mu}^{HO} > 45^\circ$. However, the two μ -complementary values of θ_{23} lie on opposite sides of 45.75° . Since

$$\begin{aligned} \sin \theta_{\mu\mu}^{LO} &= \sin \theta_{23}^{LO} \cos \theta_{13} \text{ and} \\ \sin \theta_{\mu\mu}^{HO} &= \cos \theta_{\mu\mu}^{LO} = \sin \theta_{23}^{HO} \cos \theta_{13} , \end{aligned}$$

one can eliminate $\theta_{\mu\mu}^{LO}$ between these two equations. This gives us

$$\sin \theta_{23}^{HO} = \sqrt{\frac{1}{\cos^2 \theta_{13}} - \sin^2 \theta_{23}^{LO}} , \quad (11)$$

which is a handy equation to switch from one octant to another. For example, if $\theta_{23}^{LO} = 40^\circ$, this equation tells us that the corresponding value of θ_{23}^{HO} is 51.54° .

We can try to recast Eq. 11 in terms of deviations from maximality, rather than in terms of the angles themselves. To this end, we define

$$\delta_{23}^{LO/HO} = \theta_{23}^{LO/HO} - 45^\circ .$$

Assuming small deviations, we can linearize Eq. 11. This gives us

$$\delta_{23}^{HO} = \sin^2 \theta_{13} - \delta_{23}^{LO} = 1.43^\circ - \delta_{23}^{LO} , \quad (12)$$

which implies

$$\theta_{23}^{HO} = 91.43^\circ - \theta_{23}^{LO} . \quad (13)$$

We will use these relations to interpret the results of our simulations.

In Ref. [30], the authors have argued that a precise measurement of θ_{23} is difficult in the vicinity of 45° because $\sin^2 2\theta_{23}$ attains a maximum here, making $\Delta(\sin^2 2\theta_{23})$ very small. Therefore it is worth discussing whether this θ_{13} -effect can have experimentally observable consequences. In order to directly observe a shift of 0.75° at $\theta_{\mu\mu} = 45^\circ$ ($\theta_{23} = 45.75^\circ$), we need a precision of 0.001 in our measurement of $\sin^2 2\theta_{23}$. This is far beyond our experimental reach. However, if $\theta_{\mu\mu}^{LO} = 40^\circ$ ($\theta_{23}^{LO} = 40.63^\circ$), the precision in $\sin^2 2\theta_{23}$ required to observe this shift is around 0.007, which may be achievable at future facilities. Moreover, this effect can be felt indirectly, as an artificially enhanced/reduced sensitivity in oscillation experiments. We illustrate this through simulations, in the next section.

III. SIMULATIONS

As we have mentioned before, our aim is to illustrate the difference between choosing the ‘wrong’ definition: $\theta_{23} = \theta_{\mu\mu}$ and the ‘right’ definition: $\theta_{23} = \sin^{-1}(\sin \theta_{\mu\mu} / \cos \theta_{13})$. In order to show the experimentally observable effects of this choice, we have simulated the NO ν A experiment using the GLoBES package [17, 31–36]. In this section, we discuss the results of our simulations.

We have used the standard NO ν A setup [17], with a 14 kton totally active scintillator detector placed 810 km away from the NuMI beam at a 14 mrad off-axis location. The beam, with a power of 0.7 MW, is assumed to run for three years each with neutrinos and

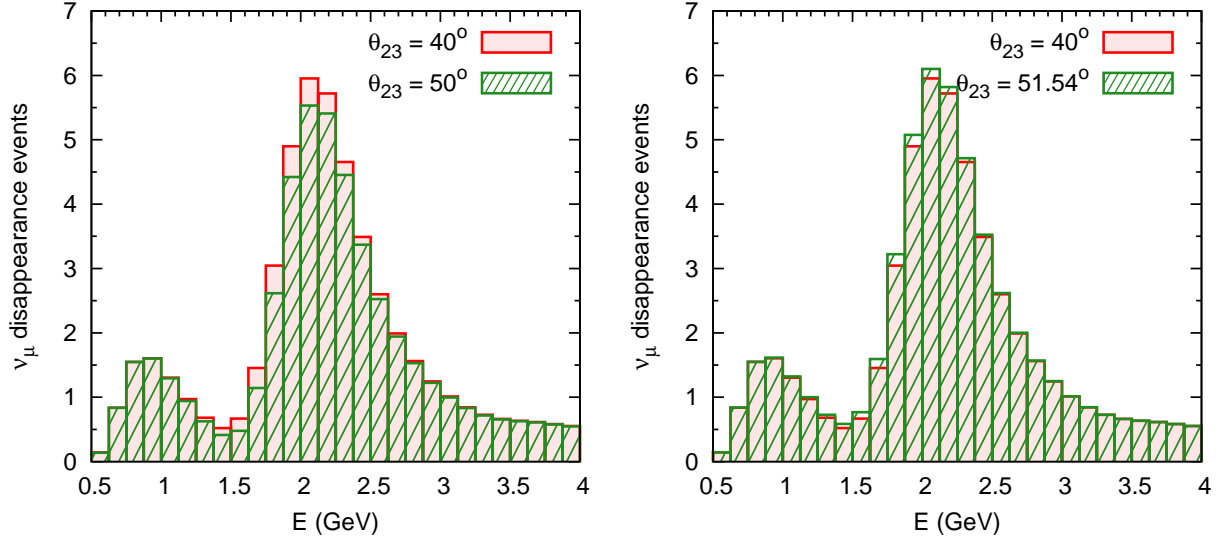


FIG. 2: ν_μ disappearance event rates for $\theta_{23}^{LO} = 40^\circ$ are shown as a solid (red) histogram in both panels. Superimposed on this, as a hatched (green) histogram are the event rates for the corresponding θ_{23}^{HO} using the ‘wrong’ definition (left panel) and ‘right’ definition (right panel). For the ‘right’ definition, the event rates show a good match.

antineutrinos. We have taken the energy resolution for ν_μ to be $0.06\sqrt{E(\text{GeV})}$ [36]. Backgrounds from NC events have also been taken into account. For the oscillation parameters, we have chosen $\sin^2 \theta_{12} = 0.304$, $\sin^2 2\theta_{13} = 0.1$, $\Delta_{21} = 7.6 \times 10^{-5} \text{ eV}^2$, $\Delta_{\mu\mu} = 2.4 \times 10^{-3} \text{ eV}^2$ and $\delta_{CP} = 0$, unless specified otherwise.

In Fig. 2, we have plotted the event rates from the muon disappearance channel. In the left panel, we have chosen the ‘wrong’ definition of θ_{23} , so that $\theta_{23}^{LO} = 40^\circ$ implies $\theta_{23}^{HO} = 50^\circ$. This gives us a difference in the number of events. However, on using the ‘right’ definition ($\theta_{23}^{HO} = 51.54^\circ$), we find that the event rates match, as seen in the right panel.

Having showed the difference due to our choice of θ_{23} at the event level, we now proceed to do so at the level of χ^2 . Throughout our simulations, we have used the values specified above as the true values of oscillation parameters. We have varied the test values of the parameters in the following ranges: $\sin^2 2\theta_{13} \in [0.07, 0.13]$, $\theta_{\mu\mu} \in [35^\circ, 55^\circ]$, $|\Delta_{\mu\mu}| \in [2.05, 2.75] \times 10^{-3} \text{ eV}^2$ and $\delta_{CP} \in [0, 2\pi)$. The solar parameters Δ_{21} and θ_{12} have been kept fixed in this analysis, since the effect of their variation is small. The mass hierarchy is assumed to be normal.

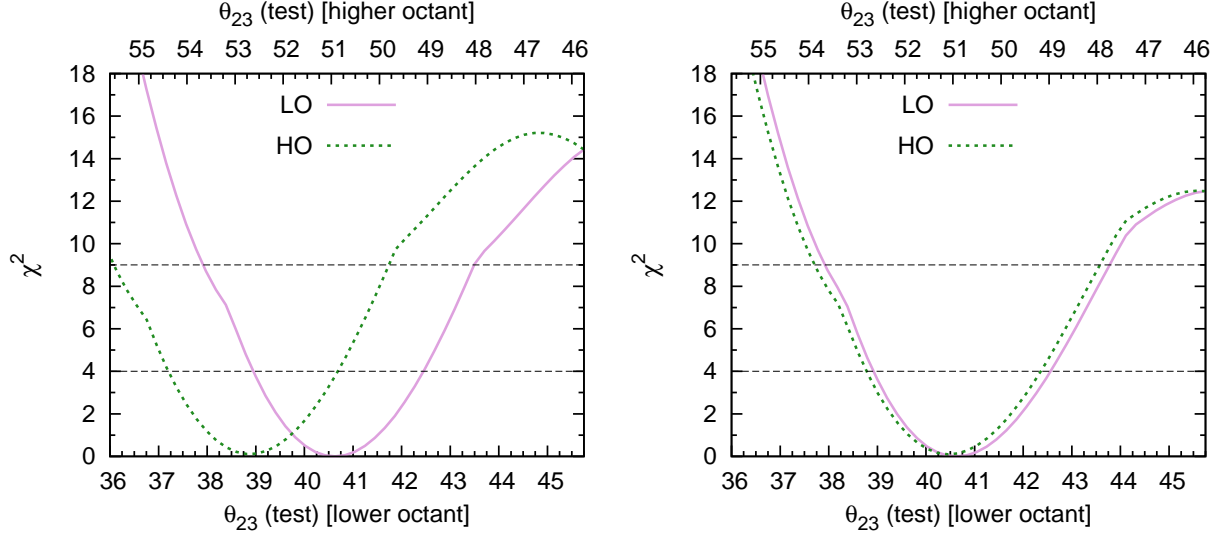


FIG. 3: χ^2 for sensitivity to the value of θ_{23} from muon disappearance from NO ν A . True $\theta_{\mu\mu} = 40^\circ$. The solid (pink) curve gives χ^2 for test $\theta_{\mu\mu}$ in the lower octant (read the lower x-axis), while the dotted (green) curve gives χ^2 for test $\theta_{\mu\mu}$ in the higher octant (read the upper x-axis). In the left panel, we have chosen the ‘wrong’ definition of θ_{23} while in the right panel we have chosen the ‘right’ definition of θ_{23} .

In Fig. 3, we have plotted the sensitivity to θ_{23} for true $\theta_{\mu\mu} = 40^\circ$. As the test value of $\theta_{\mu\mu}^{LO}$ increases in the lower (true) octant from 35° to 45° , θ_{23}^{LO} increases from 35.53° to 45.75° . This range is shown on the lower x-axis. Correspondingly, θ_{23}^{HO} decreases from 55.60° to 45.75° . This range, for the higher (false or degenerate) octant, is shown on the upper x-axis. The advantage of using these double-axes is that values of θ_{23} along a vertical line are μ -complementary . We have used the linearized relation in Eq. 13 to plot these axes. For values of test $\theta_{\mu\mu}$ in the lower octant, χ^2 has been plotted as the solid (pink) curve. The lower x-axis should be used to read the θ_{23} values for this curve. For values of test $\theta_{\mu\mu}$ in the higher octant, χ^2 has been plotted as the dotted (green) curve. The upper x-axis should be used to read the θ_{23} values for this curve.

The following features are visible in Fig. 3: (a) For $\theta_{\mu\mu} = 40^\circ$, the best-fit point is seen at the corresponding value of θ_{23} which is 40.63° (b) If we use the ‘wrong’ definition of θ_{23} , the minima in the two octants do not appear for μ -complementary values of θ_{23} . This is seen in the left panel. In the right panel, we have used the ‘right’ definition. As a result, we find that the minima coincide. (c) The sensitivities in the two octants coincide at $\theta_{23} = 45.75^\circ$,

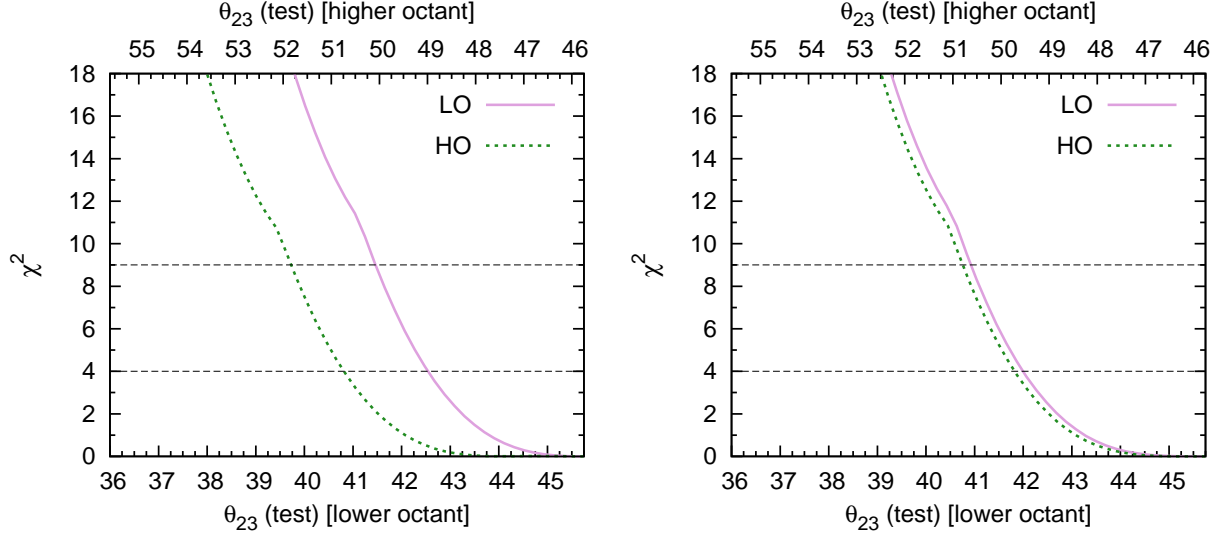


FIG. 4: χ^2 for sensitivity to the value of θ_{23} from muon disappearance from NO ν A . True $\theta_{\mu\mu} = 45^\circ$. The solid (pink) curve gives χ^2 for test $\theta_{\mu\mu}$ in the lower octant (read the lower x-axis), while the dotted (green) curve gives χ^2 for test $\theta_{\mu\mu}$ in the higher octant (read the upper x-axis). In the left panel, we have chosen the ‘wrong’ definition of θ_{23} while in the right panel we have chosen the ‘right’ definition of θ_{23} .

rather than $\theta_{23} = 45^\circ$. This is expected from the analytic calculations presented in the previous section.

Figure 4 is similar to Fig. 3, but with true $\theta_{\mu\mu} = 45^\circ$. Note that compared to the ‘right’ definition χ^2 , the ‘wrong’ definition χ^2 is more in the lower octant, and less in the higher octant. Clearly, using the ‘wrong’ definition gives us an incorrect value of χ^2 . Thus, if χ^2 from the ‘wrong’ definition is used to set a prior on θ_{23} for future experiments, it will give a spurious indication of the confidence with which certain θ_{23} values are allowed. This also has implications for octant sensitivity studies. Since θ_{23} and $90^\circ - \theta_{23}$ are not μ -complementary, $\chi^2(\theta_{23}; 90^\circ - \theta_{23})$ does not give the correct octant sensitivity. Therefore, care must be taken to use the ‘right’ definition in simulations.

Finally, in Fig. 5, we have plotted the allowed values of θ_{23} for all possible true values of θ_{23} in the range $[36^\circ, 55^\circ]$. For each true value, the allowed test values can be read from its corresponding vertical line. The 68%, 90% and 95% C.L. contours are also shown. For a given true value of θ_{23} , we find an allowed range of test θ_{23} in each octant. For the ‘right’ definition, we see that the false degenerate solution lies along the line $\theta_{23}^{HO} = 91.43^\circ - \theta_{23}^{LO}$

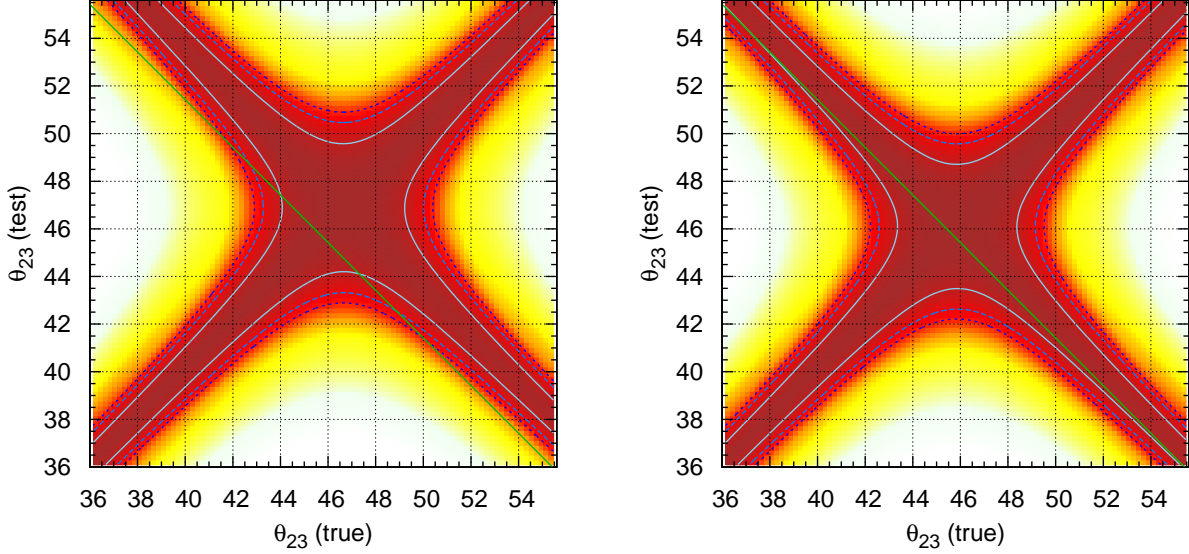


FIG. 5: Allowed test values for θ_{23} (y-axis) in degrees, for a given true value of θ_{23} (x-axis). 68%, 90% and 95% C.L. contours are also shown. As before, the left(right) panel is plotted using the ‘wrong(right)’ definition of θ_{23} . With the ‘right’ definition, we see the expected behaviour - the false degenerate solution lies along the line $\theta_{23}^{HO} = 91.43^\circ - \theta_{23}^{LO}$ (shown by the straight diagonal (green) line).

(Eq. 13). But if we choose the ‘wrong’ definition, then we get degenerate solutions that are not μ -complementary, along with incorrect values of χ^2 .

In this paper, we have only presented the results for the case where NH is the true hierarchy, and true $\delta_{CP} = 0$. However, we have verified that these results hold for IH, and for a number of values of δ_{CP} .

IV. CONCLUSIONS AND SUMMARY

In this study, we have discussed the effect of three-flavour mixing on our measurement of θ_{23} . We have calculated the relation between the value of θ_{23} in nature, and $\theta_{\mu\mu}$ that is measured in muon disappearance experiments. The difference between these two numbers is significant, in light of the measured value of θ_{13} . Using the ‘right’ definition of θ_{23} (incorporating the θ_{13} -effect), we have found the allowed values of θ_{23} in the two octants, corresponding to a single measured value of $\sin^2 2\theta_{\mu\mu}$. We know that complementary values of $\theta_{\mu\mu}$ in the two octants are related by $\theta_{\mu\mu}^{HO} = 90^\circ - \theta_{\mu\mu}^{LO}$. But for a given measurement of $\sin^2 2\theta_{\mu\mu}$, we have found that the corresponding values of θ_{23} in the two octants are related

by $\theta_{23}^{HO} = 91.43^\circ - \theta_{23}^{LO}$. We have called this relation μ -complementarity. The exact form of this equation comes from the value of θ_{13} .

Through simulations, we have showed that using the ‘wrong’ definition gives us degenerate fits at non- μ -complementary values of θ_{23} . Consequently, the muon disappearance analysis can give an incorrect prior on θ_{23} . In determining octant sensitivity, if the ‘wrong’ definition is used, one can get an incorrect value of χ^2 . Therefore, we advocate the use of the ‘right’ definition (as given in Eq. 10) for calculating the oscillation probability in simulations. However, priors from previous experiments should be added in terms of $\sin^2 2\theta_{\mu\mu}$ – the quantity that is measured in the muon disappearance experiments. Our results and conclusions have been found to hold true for both hierarchies and for values of δ_{CP} in its entire allowed range.

Acknowledgments

The author would like to thank Srubabati Goswami and S. Uma Sankar for useful discussions, and for a critical reading of the manuscript.

-
- [1] X. Guo et al. (Daya-Bay) (2007), hep-ex/0701029.
 - [2] F. Ardellier et al. (2004), hep-ex/0405032.
 - [3] F. Ardellier et al. (Double Chooz) (2006), hep-ex/0606025.
 - [4] S.-B. Kim (RENO), AIP Conf. Proc. **981**, 205 (2008).
 - [5] D. G. Michael et al. (MINOS), Phys. Rev. Lett. **97**, 191801 (2006), hep-ex/0607088.
 - [6] Y. Itow et al. (T2K) (2001), hep-ex/0106019.
 - [7] F. An et al. (DAYA-BAY Collaboration), Phys.Rev.Lett. **108**, 171803 (2012), arXiv:1203.1669.
 - [8] Y. Abe et al. (DOUBLE-CHOOZ Collaboration), Phys.Rev.Lett. **108**, 131801 (2012), arXiv:1112.6353.
 - [9] J. Ahn et al. (RENO collaboration), Phys.Rev.Lett. **108**, 191802 (2012), arXiv:1204.0626.
 - [10] G. Fogli, E. Lisi, A. Marrone, D. Montanino, A. Palazzo, et al. (2012), arXiv:1205.5254.
 - [11] D. Forero, M. Tortola, and J. Valle (2012), arXiv:1205.4018.
 - [12] M. Gonzalez-Garcia, M. Maltoni, J. Salvado, and T. Schwetz (2012), arXiv:1209.3023.

- [13] X. Qian (Daya Bay) (2012), talk given at the NuFact 2012 Conference, July 23-28, 2012, Williamsburg, USA, <http://www.jlab.org/conferences/nufact12/>.
- [14] Q. R. Ahmad et al. (SNO), Phys. Rev. Lett. **87**, 071301 (2001), nucl-ex/0106015.
- [15] K. Eguchi et al. (KamLAND), Phys. Rev. Lett. **92**, 071301 (2004), hep-ex/0310047.
- [16] A. Holin (MINOS Collaboration), PoS **EPS-HEP2011**, 088 (2011), arXiv:1201.3645.
- [17] D. Ayres et al. (NOvA Collaboration) (2007).
- [18] V. Barger, D. Marfatia, and K. Whisnant, Phys. Rev. **D66**, 053007 (2002), hep-ph/0206038.
- [19] P. Huber, M. Lindner, T. Schwetz, and W. Winter, JHEP **11**, 044 (2009), arXiv:0907.1896.
- [20] S. Prakash, S. K. Raut, and S. U. Sankar, Phys.Rev. **D86**, 033012 (2012), arXiv:1201.6485.
- [21] T. Akiri et al. (LBNE Collaboration) (2011), arXiv:1110.6249.
- [22] P. Coloma, T. Li, and S. Pascoli (2012), arXiv:1206.4038.
- [23] S. Fukuda et al. (Super-Kamiokande), Phys. Lett. **B539**, 179 (2002), hep-ex/0205075.
- [24] R. Gandhi et al., Phys. Rev. **D76**, 073012 (2007), arXiv:0707.1723.
- [25] J.-E. Campagne, M. Maltoni, M. Mezzetto, and T. Schwetz, JHEP **04**, 003 (2007), hep-ph/0603172.
- [26] V. Barger, D. Marfatia, and K. Whisnant, Phys.Rev. **D65**, 073023 (2002), hep-ph/0112119.
- [27] C. Lam, Phys.Lett. **B507**, 214 (2001), hep-ph/0104116.
- [28] H. Nunokawa, S. J. Parke, and R. Zukanovich Funchal, Phys.Rev. **D72**, 013009 (2005), hep-ph/0503283.
- [29] A. de Gouvea, J. Jenkins, and B. Kayser, Phys.Rev. **D71**, 113009 (2005), hep-ph/0503079.
- [30] H. Minakata, M. Sonoyama, and H. Sugiyama, Phys.Rev. **D70**, 113012 (2004), hep-ph/0406073.
- [31] P. Huber, M. Lindner, and W. Winter, Comput. Phys. Commun. **167**, 195 (2005), hep-ph/0407333.
- [32] P. Huber, J. Kopp, M. Lindner, M. Rolinec, and W. Winter, Comput. Phys. Commun. **177**, 432 (2007), hep-ph/0701187.
- [33] T. Yang and S. Wojcicki (NOvA) (2004), Off-Axis-Note-SIM-30.
- [34] M. D. Messier (1999), ph.D. Thesis (Advisor: James L. Stone).
- [35] E. Paschos and J. Yu, Phys.Rev. **D65**, 033002 (2002), hep-ph/0107261.
- [36] R. Patterson (NO ν A) (2012), talk given at the Neutrino 2012 Conference, June 3-9, 2012, Kyoto, Japan, <http://neu2012.kek.jp/>.